



# MCP-based detectors: calibration and first photon radiation measurements<sup>1</sup>

Evgeny Syresin,<sup>a</sup> Alexander Grebentsov,<sup>a\*</sup> Oleg Brovko,<sup>a</sup> Mikhail Yurkov,<sup>b</sup> Wolfgang Freund<sup>c</sup> and Jan Grünert<sup>c</sup>

<sup>a</sup>Joint Institute for Nuclear Research (JINR), Joliot-Curie 6, Dubna, Moscow Region 141980, Russian Federation, <sup>b</sup>Deutsches Elektronen Synchrotron (DESY), Notkestraße 85, 22603 Hamburg, Germany, and <sup>c</sup>European XFEL, Holzkoppel 4, 22869 Schenefeld, Germany. \*Correspondence e-mail: grebentsov@jinr.ru

Received 28 November 2018

Accepted 3 May 2019

Edited by G. Grübel, HASYLAB at DESY, Germany

<sup>1</sup>This article will form part of a virtual special issue containing papers presented at the PhotonDiag2018 workshop.

**Keywords:** XFEL physics; photon beam diagnostics; microchannel plate detectors.

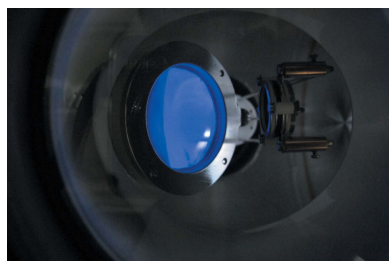
Detectors based on microchannel plates (MCPs) are used to detect radiation from free-electron lasers. Three MCP detectors have been developed by JINR for the European XFEL (SASE1, SASE2 and SASE3 lines). These detectors are designed to operate in a wide dynamic range from the level of spontaneous emission to the SASE saturation level (between a few nJ up to 25 mJ), in a wide wavelength range from 0.05 nm to 0.4 nm for SASE1 and SASE2, and from 0.4 nm to 4.43 nm for SASE3. The detectors measure photon pulse energies with an anode and a photodiode. The photon beam image is observed with an MCP imager with a phosphor screen. At present, the SASE1 and SASE3 MCP detectors are commissioned with XFEL beams. Calibration and first measurements of photon radiation in multibunch mode are performed with the SASE1 and SASE3 MCPs. The MCP detector for SASE2 and its electronics are installed in the XFEL tunnel, technically commissioned, and are now ready for acceptance tests with the X-ray beam.

## 1. Introduction

Radiation detectors based on microchannel plates (MCPs) (Syresin *et al.*, 2011; Brovko *et al.*, 2012) have been installed at the European XFEL (EuXFEL). An important task of photon beam diagnostics at the EuXFEL (Grünert, 2009) is providing reliable tools for measurements aimed at searching for and fine-tuning of the free-electron-laser (FEL) creating SASE (self-amplified spontaneous emission) process. The problem of detecting SASE amplification is crucial for XFELs because of the large synchrotron radiation background. The detectors operate over a wide dynamic range from the level of spontaneous emission to the saturation level, and over a wide wavelength range.

Three MCP devices have been installed at the EuXFEL facility (Sinn *et al.*, 2011), one after each SASE undulator (SASE1, SASE2 and SASE3). Three different tasks can be fulfilled with the XFEL MCP-based photon detectors: study of the initial stage of the SASE regime, measurement of the photon pulse energy, and measurement of the photon beam image. The MCP detector will resolve each individual pulse at a repetition rate of 4.5 MHz. The MCP-based photon detectors will allow:

- (i) Measurement of the pulse energy.
- (ii) Measurement of the photon beam image.
- (iii) Operation at the pulse repetition rate of the XFEL (bunch train repetition rate of 10 Hz, intra-bunch train repetition rate of 4.5 MHz), thus resolving each individual radiation pulse.



(iv) A pulse energy measurement relative accuracy better than 1%.

(v) A photon pulse energy dynamic range from a few nJ up to 25 mJ; this applies to spontaneous and FEL radiation.

(vi) Visualization with the MCP imager of a single bunch in a train, or an average image over the full train.

## 2. Design of the MCP detector

The SASE1 and SASE2 MCP detectors (Fig. 1) are almost identical. They consist of two ports: three MCPs equipped with the anode as a pulse energy monitor, and one MCP detector for imaging the photon beam and a semiconductor photo-detector.

The first MCP detector port houses two Hamamatsu F4655 MCPs, 18 mm in diameter (Fig. 2), which are used for measuring the pulse energy and searching for initial indications of the SASE regime. The Si PIN photodiode (Hamamatsu S3590) that is installed in this port detects X-ray radiation from the undulator. The MCPs and the photodiode installed in the first port of the MCP detector are shown in Fig. 2. The PM 100-250 3D vacuum manipulator moves these detectors in the horizontal direction through a distance of 200 mm ( $x$  axis); the vertical displacement range is  $\pm 20$  mm

( $y$  axis) relative to the beam axis. It permits a considerable increase in the vertical size of the SASE regime search area in comparison with the MCP diameter. The linear motions of the detectors are executed by stepper motors (Baur\_PI\_Motor SM224M-K and SM234M-K).

The second detector port houses one Hamamatsu F4655 MCP for measurement of the pulse energies and the beam observation system (BOS-40-IDA-CH/P-47) that has a 40 mm diameter of active MCP area and a P-47 phosphor screen (Fig. 3). These MCPs are also moved in the horizontal direction over a distance of 200 mm (along the  $x$  axis) and in the vertical direction  $\pm 20$  mm ( $y$  axis) relative to the photon beam axis. The BOS MCP is set at an angle of  $45^\circ$  with respect to the photon beam and a viewport is used to provide the best imaging on a CCD.

To search for the SASE mode, a CCD camera (Basler avA1600-50gm) with a large field of view of about 90 mm diameter (MCP diameter of 40 mm and a vertical displacement of  $\pm 20$  mm) and a relatively small number of pixels per millimetre is installed in the second port of the MCP detector for recording the phosphor screen image (Fig. 4).

The SASE3 MCP detector has the same ports as the SASE1/SASE2 detectors and also an additional port with three movable semi-transparent wire meshes made from nickel (2% open area) and stainless steel (79% and 88% open area) for the production of scattering FEL radiation, similar to

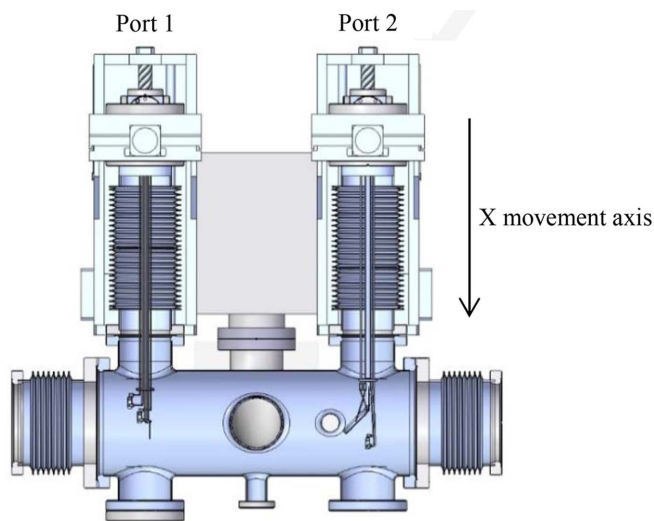


Figure 1  
Top view of the SASE1 MCP detector.

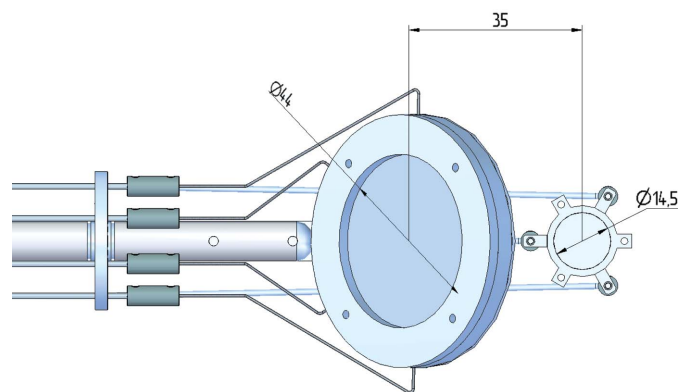


Figure 3  
Second port with a BOS MCP imager and Hamamatsu F4655 MCP.

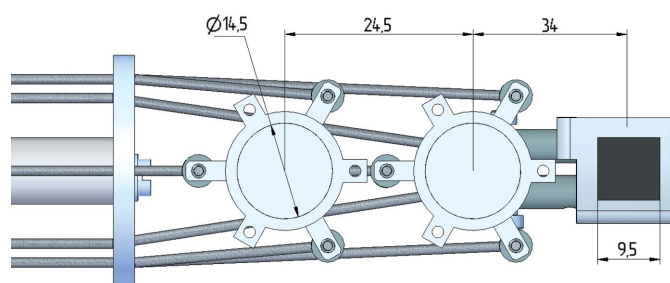


Figure 2  
First port with two Hamamatsu F4655 MCPs and one Hamamatsu S3590 photodiode.

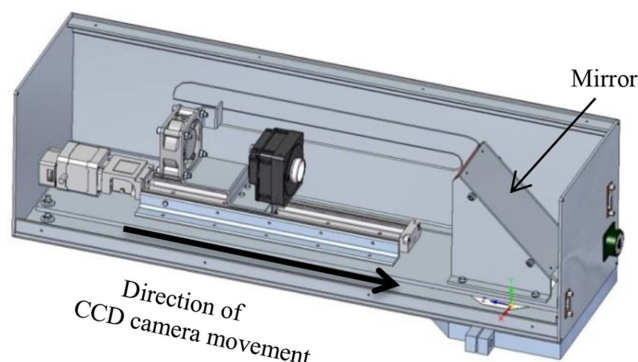


Figure 4  
Camera box with a CCD Basler camera.

those used at FLASH. The MCP quantum efficiency for photons at  $\lambda = 0.4\text{--}4.4\text{ nm}$  is about 5–30%. The mesh attenuation system operates well at FLASH for the minimum wavelength of 4 nm.

### 3. MCP detector tests

#### 3.1. MCP acceptance tests

The acceptance tests for precise positioning and movements of the detectors inside the vacuum chamber were performed with an optical laser positioner for the SASE1 unit. The laser beam was directed by the MCP BOS system at different incident angles and positions. This procedure was fully analogous to recording XFEL radiation at an incidence angle variation of the carbon mirrors installed upstream of the MCP-based detector. At each laser beam incident angle, the MCP BOS system was moved into a position where the laser spot was observed in the center of the phosphor screen. The  $x$  and  $y$  coordinates at the center of the laser spot were measured. Information about these coordinates was stored in the control software system to correct the positions of the MCP1–MCP3 pulse energy monitors relative to the X-ray beam. The simulated detector coordinates were used for movement of the MCP pulse energy monitors to new coordinates  $x_1$  and  $y_1$ . The procedure of searching for XFEL irradiation was successfully tested with the application of the laser positioner.

Operability of the small MCP detectors was verified with signals from the direct and reflected radiation of a UV lamp (Fig. 5). Operability of the photodiode was checked using the photovoltaic effect directly without any bias voltage.

Operability of the BOS MCP with a phosphor screen (Fig. 6) is determined by the glow of the phosphor screen under the action of UV radiation.

Movement tests were carried out with a control crate, which included Beckhoff and Technosoft controllers for the  $x$  and  $y$  axis motors and the camera motor. Alignment of the CCD camera box (SASE1 MCP detector) was carried out during the final tests.

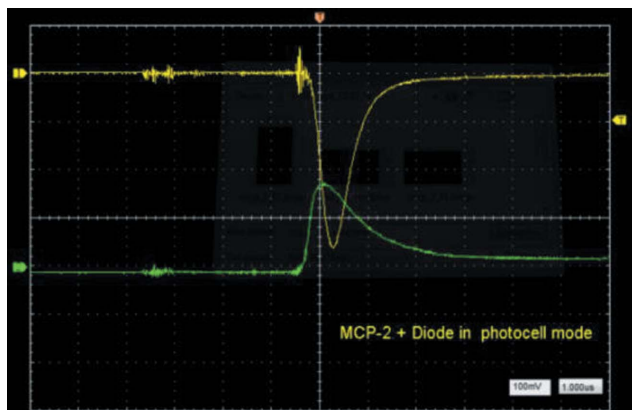


**Figure 5** MCP2 and photodiode signals produced by the flash lamp (SASE1 MCP detector).

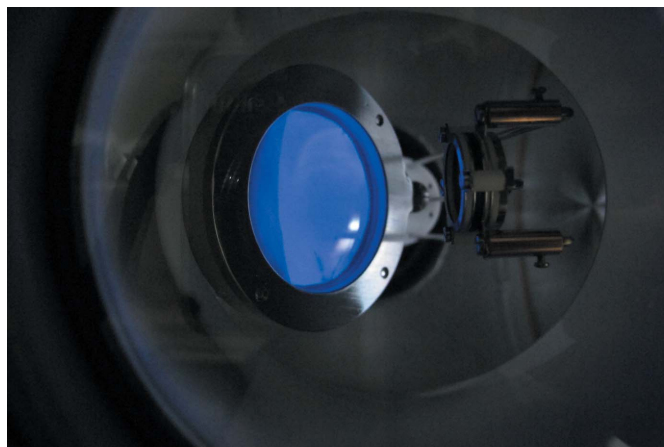


**Figure 6** SASE1 BOS MCP glow under the action of UV radiation.

The SASE1, SASE2 and SASE3 MCP detectors were installed in the EuXFEL tunnels after calibration and acceptance tests.

#### 3.2. Test experiment with MCP

Prior to their installation at the EuXFEL, the MCP SASE1 detectors were calibrated using radiation with wavelengths lying in the UV and X-ray ranges. A lamp generating UV radiation was used for calibration in this wavelength range. The dependence of the MCP gain on the applied high voltage is shown in Fig. 7. As the applied high voltage is varied from 1.5 kV to 2.1 kV the gain is increased by four orders of magnitude. Note that the spatial charge effects play a significant role in the MCP channels at voltages below 1.4 kV. This voltage value is a minimum for the F4655 MCP.

Further experiments with the SASE1 MCP were conducted in the X-ray range at the DORIS synchrotron (BW1 channel; Syresin, Grebentsov *et al.*, 2014). Absolute measurements of the radiation energy  $E_r$  in a micropulse were performed with the use of the MCP and a semiconductor photodiode at  $E_r > 0.03\text{ nJ}$ , a photon energy of 8.5–12 keV and a pulse repetition time of 192 ns or 96 ns. The detectors were operated at a photon flux between  $4 \times 10^7\text{ photons s}^{-1}$  and

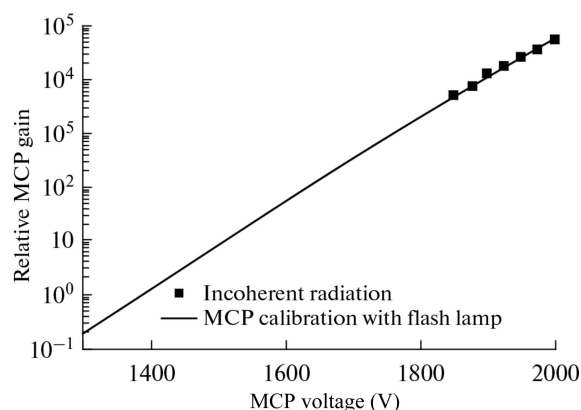


**Figure 7** Dependence of the F4655 MCP gain on the high voltage applied to it.

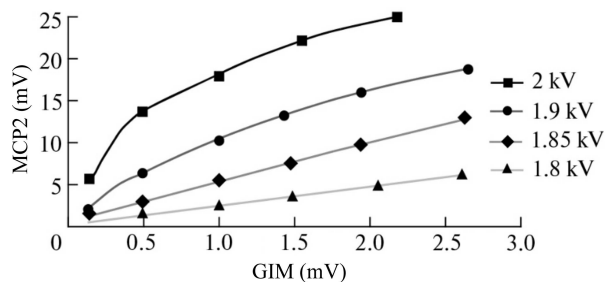


**Figure 8**  
Dependence of the MCP signal on the ionization chamber signal for various high-voltage values.

$2 \times 10^{11}$  photons  $s^{-1}$ . The pressure in the detector vacuum chamber was  $5 \times 10^{-9}$  mbar. A beryllium foil with a thickness of 200  $\mu\text{m}$  was placed at the entry to the detector vacuum chamber. The ionization chamber was positioned in front of the detector MCP input and served to measure the synchrotron radiation flux. The dependence of the MCP signal on the ionization chamber signal for a photon energy of 9.66 keV and four values of the high voltage applied to the MCP (1.8 kV, 1.85 kV, 1.9 kV and 2 kV) are shown in Fig. 8.

A pronounced influence of the secondary ions produced in the detector vacuum chamber by the ionization of residual gas atoms by the X-ray gamma quanta is observed at voltages of 1.9 kV and 2 kV. At voltages of 1.8 kV and 1.85 kV, the MCP signal increases linearly with increasing signal from the ionization chamber. The ratio of the MCP signal to the radiation energy in a micropulse is  $0.165 \text{ V nJ}^{-1}$  at a voltage of 1.8 kV and a photon energy of 9.66 keV (Syresin, Brovko *et al.*, 2014). It is expected that at XFEL radiation energies a micropulse of 1 mJ will yield an MCP signal of 1.2 V at an applied voltage of 1.5 kV.

The time structure of the synchrotron radiation micropulses was measured using the photodiode and the MCP at a repetition rate of about 10 MHz (Fig. 9).

The BOS MCP with a phosphor screen was efficiently used to search for the beam position at a synchrotron radiation intensity above  $4 \times 10^7$  photons  $s^{-1}$ . It should be noted that, due to the low contrast resolution of the screen and the broadening of the image spot on this screen, the detector provides data on the beam centroid position for beams with a transverse size smaller than 0.5 mm, but does not allow the shape of such beams to be studied.

#### 4. First experiments with the photon beam

The SASE1 and SASE3 MCP detectors were commissioned in single and multibunch modes (Figs. 10 and 11). The minimum pulse separation inside an X-ray pulse train of EuXFEL can be as short as 220 ns. The temporal reso-

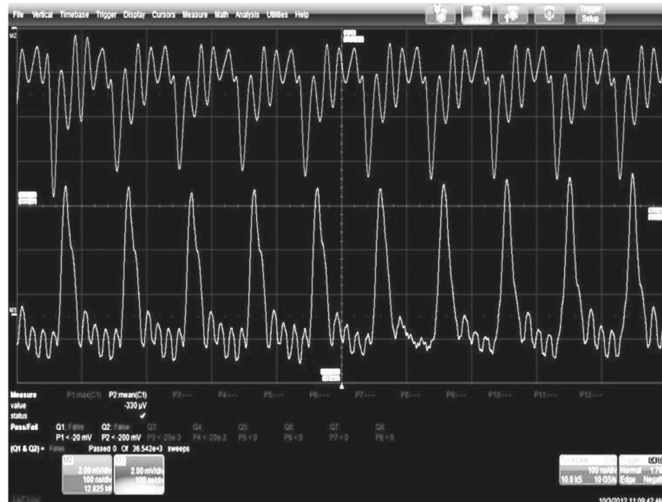


**Figure 9**  
Signal from the MCP (upper signal) and the photodiode (low signal) at a radiation pulse repetition time of 96 ns.

lution of the MCP detectors was verified for this case (4.5 MHz repetition rate) by demonstrating a clear pulse separation. The intensity in each pulse can be provided by fast digitizer electronics that operate at 125 MHz sampling.

The first experience of the SASE3 commissioning in multibunch mode is shown in Fig. 11 for the following regime: 30 bunches per train, only the minimal number of undulator segments (12) closed for lasing, low-intensity SASE (X-ray gas monitor shows 10  $\mu\text{J}$  in linear regime), synchrotron radiation absorber 2 mm  $\times$  2 mm, photon energy of 930 eV and electron energy of 14 GeV. The MCP2 (SASE3) can detect radiation scattered from the offset mirrors and thus operate parasitically.

The peculiarity of the SASE XFEL MCP measurement is the large synchrotron radiation background at an electron energy of 14 GeV. An MCP image of the SASE signal (red circular spot) and an image of the background synchrotron radiation (rectangular spot) are shown in Fig. 12.

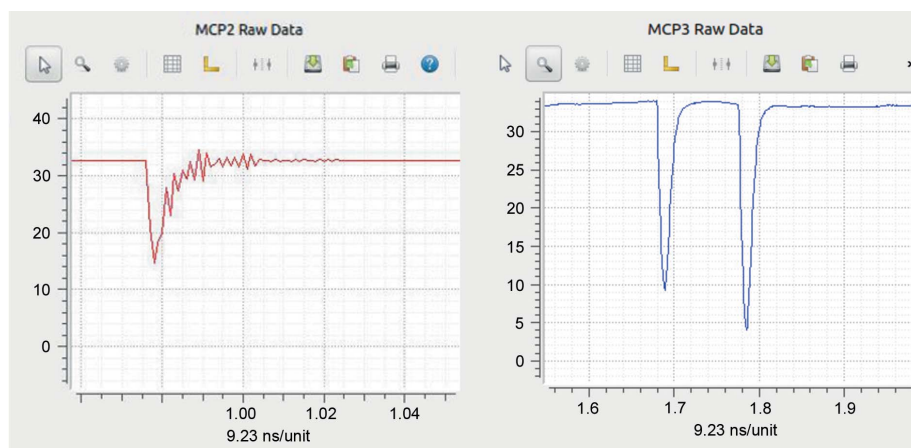


**Figure 10**  
SASE3 MCP2 and SASE2 MCP3 detectors, beam tests with single-bunch and two-bunch mode.

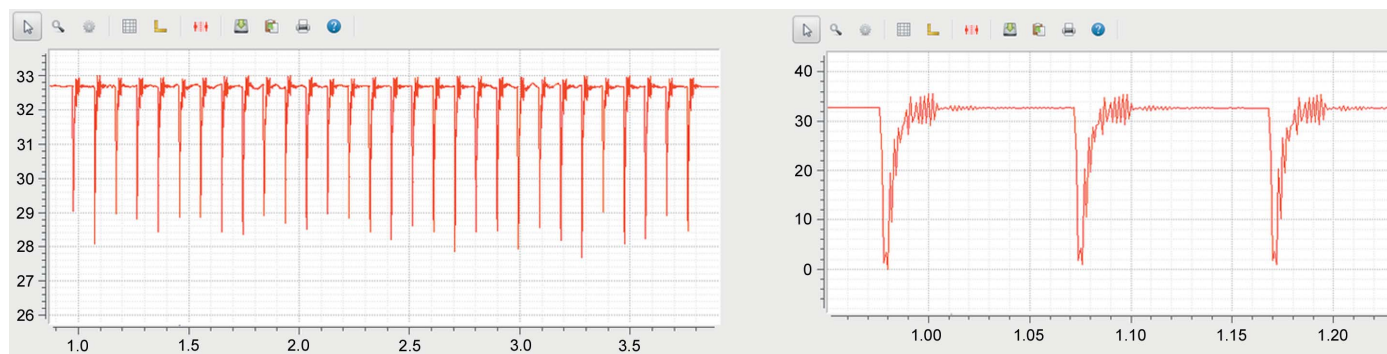


**Figure 11**  
SASE3 MCP in multi-bunch mode: 30 bunches per train and the first three bunches.

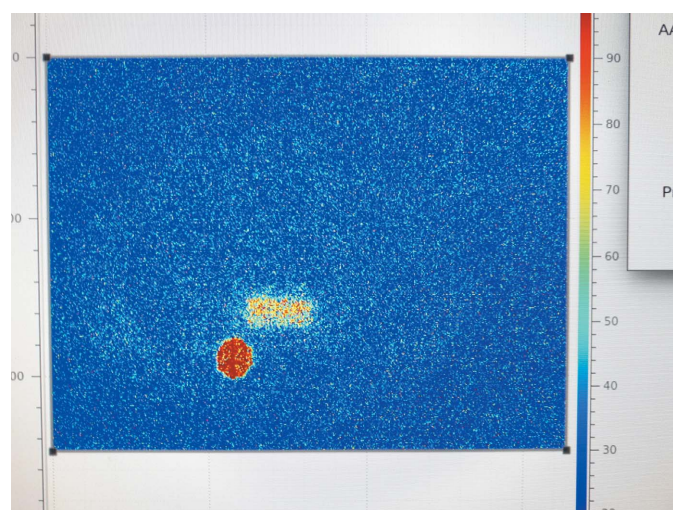


**Figure 12**  
BOS MCP image measurements at an electron energy of 14 GeV.

Absolute intensity values of SASE radiation can be obtained through cross-calibration with X-ray gas monitors (XGMs) (Grünert *et al.*, 2015), which can be operated simultaneously with MCP-based detectors (Fig. 13). There are six XGMs at the EuXFEL that provide online beam position and intensity radiation monitoring. The XGM consists of four vacuum chambers placed on a common girder, and can record the fast shot-to-shot beam position and intensity as well as the absolute calibrated intensity.

### 5. Conclusions

Successful operation of a FEL strongly depends on the quality of the radiation detectors. XFEL MCP detectors operate in a wide dynamic range from a few nJ up to 25 mJ, and in a wide wavelength range from 0.05 nm to 0.4 nm for SASE1 and SASE2, and from 0.4 nm to 4.43 nm for SASE3. An essential feature of the detectors is a high relative accuracy of measurements

(below 1%), which is crucial for detection of a signature of amplification and characterization of statistical properties of the radiation. MCP detectors with these unique characteristics will be used as key instrumentation for the tuning of an XFEL accelerator and searching of SASE regimes. Other diagnostic tools cannot be used for the registration of XFEL radiation with such a wide dynamic range and wide wavelength range.

During validation tests at the DORIS BW1 channel, detector calibration was carried out in the X-ray range at photon energies of 8.5–12.4 keV. The ratio of the MCP signal to the radiation energy in a micropulse is  $0.165 \text{ V nJ}^{-1}$  at a voltage of 1.8 kV and a photon energy of 9.66 keV.

At present, the SASE1, SASE2 and SASE3 MCP detectors are installed in the EuXFEL tunnels (Syrekin *et al.*, 2017). The first beam time structure was measured by MCP detectors. A peculiarity of the SASE XFEL MCP measurement is a large synchrotron radiation background at an electron energy of 14 GeV. The first SASE radiation intensity measurements were performed using MCP and XGM.

### Acknowledgements

All authors acknowledge the outstanding contributions from the European XFEL support groups: X-ray Optics (XRO) led by Harald Sinn, Vacuum (VAC) led by Martin Dommach, advanced Electronics (AE) led by Patrick Gessler, Informa-

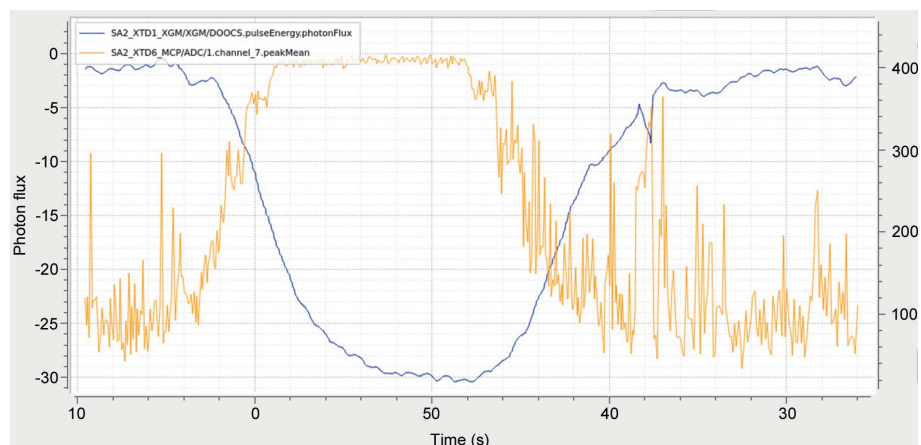


**Figure 13**  
SASE2 MCP3 (yellow) and XGM (blue) signals at EuXFEL operation.

tion Technology and Data Management (ITDM) led by Krzysztof Wrona, and Control and Analysis Software (CAS) led by Sandor Brockhauser.

## References

- Brovko, O., Grebentsov, A., Makarov, R., Morozov, N., Shabunov, A., Syresin, E. & Yurkov, M. (2012). *Proceedings of the 23rd Russian Particle Accelerator Conference (RUPAC2012)*, 24–28 September 2012, Saint-Petersburg, Russia. WEPPD003.
- Grünert, J. (2009). *Proceedings of the 31st Free Electron Laser Conference (FEL2009)*, 23–28 August 2009, Liverpool, UK.
- Grünert, J., Koch, A., Kujala, N., Freund, W., Planas, M., Dietrich, F., Buck, J., Liu, J., Sinn, H., Dommach, M. & Molodtsov, S. (2015). *Proceedings of the 37th Free Electron Laser Conference (FEL2015)*, 23–28 August 2015, Daejeon, Korea, p. 764.
- Sinn, H., Gaudin, J., Samoylova, L., Trapp, A. & Galasso, G. (2011). *X-ray Optics and Beam Transport*, EuXFEL Conceptual Design Report XFEL.EU TR-2011-002 (doi:10.3204/XFEL.EU/TR-2011-002).
- Syresin, E., Brovko, O. I., Freund, W., Yu. A., Grebentsov, Grünert, J. & Yurkov, M. V. (2017). *Proceedings of the 8th International Particle Accelerator Conference (IPAC2017)*, 14–19 May 2017, Copenhagen, Denmark, pp. 4031–4033. THPAB132.
- Syresin, E., Brovko, O., Grebentsov, A., Zamjatin, N., Shabunov, A., Yurkov, M., Gruenert, J., Freund, W., Novikov, D., Basta, R., Fiala, T. & Hedbavny, P. (2014). *Phys. Part. Nucl. Lett.* **11**, 730–736.
- Syresin, E., Brovko, O., Kapishin, M., Shabunov, A., Yurkov, M., Freund, W., Gruenert, J. & Sinn, H. (2011). *Proceedings of the 2nd International Particle Accelerator Conference (IPAC2011)*, 4–9 September 2011, San Sebastian, Spain.
- Syresin, E., Grebentsov, A., Shabunov, A., Zamiatin, N., Basta, R., Fiala, T., Hedbavny, P., Brovko, O., Freund, W., Grünert, J., Sinn, H., Novikov, D. & Yurkov M. (2014). *Proceedings of the 5th International Particle Accelerator Conference (IPAC2014)*, 15–20 June 2014, Dresden, Germany, pp. 2180–2182.